FACTA UNIVERSITATIS
Series: **Physics, Chemistry and Technology** Vol. 20, Nº 1, 2022, pp. 67 - 77
https://doi.org/10.2298/FUPCT2201067M

Original scientific paper

INFLUENCE OF NON-IRRADIATED SURFACE OPTICAL ABSORBER ON TEMPERATURE GRADIENT INDUCED BY PHOTOTHERMAL EFFECT IN A THIN FILM

UDC 536.2 + 536.5 + 536.6 + 534.6 + 535.3

Vesna Miletić[1], Marica Popović[2], Slobodanka Galović[3], Dragan Markushev[2], Ljiljana Kostić[4], Miroljub Nešić[3]

[1]University of East Sarajevo, Faculty of Philosophy – Pale, Sarajevo
[2]University of Belgrade, Institute of Physics – Zemun,
National Institute of the Republic of Serbia, Belgrade
[3]University of Belgrade, Vinča Institute of Nuclear Sciences,
National Institute of the Republic of Serbia, Belgrade
[4]University of Niš, Faculty of Sciences and Mathematics – Department of Physics, Niš

Abstract. *This paper presents the model of surface temperature variations, resulting from the photothermal effect induced in a "thin film – highly absorbing surface layer" structure, where the thin film is irradiated. The influence of the optical absorption coefficient and sample thickness on the induced temperature gradient is analyzed. It is shown that, depending on the product of these parameters (optical absorbance) in the described structure, the phenomenon of inverse temperature gradient can occur, further influencing the direction and the magnitude of thermoelastic displacement.*

Key words: *Photothermal response, photoacoustic, thermoelastic bending, low-absorbance samples*

1. INTRODUCTION

Interaction between the examined material and the excitation electromagnetic (EM) radiation is initiated by partial absorption of excitation energy, whereas a portion of it is converted into heat. This effect (of optical heating of the sample) is called the photothermal effect, and it represents the basis for a set of non-destructive material characterization methods (so-called photothermal methods), the most widely spread of which is photoacoustics

Received: October, 25th, 2022; accepted: December, 27th, 2022
Corresponding author: Vesna Miletić, Faculty of Philosophy – Pale, University of East Sarajevo, Sarajevo
E-mail: vesna.miletic@ff.ues.rs.ba

(Park et al., 1995; Rosencwaig and Gersho, 1975, 1976; Sablikov and Sandomirskii, 1983; Tam, 1986; Vargas and Miranda, 1988).

Photothermal (PT), and consequently photoacoustic (PA) techniques, are based on direct or indirect measurement of phenomena resulting from heat transfer processes in the examined material, whereas the most straightforward approach considers the examination of surface temperature variations of the sample (Popovic et al., 2018, 2021). Since these experimental techniques are considered model-dependent, their development largely involves the development and the analysis of theoretical-mathematical models which link physical processes in the examined material and the measured signal (Dramićanin et al., 2000; Galovic et al., 2003, 2014; Galović and Dramićanin, 1999; Galovic and Kostoski, 2003; Markushev et al., 2019; Nesic et al., 2016; Nesic, Galovic, et al., 2012; Nesic, Gusavac, et al., 2012; Popovic et al., 2021)(Aleksić et al., 2022; Djordjevic et al., 2022; Markushev et al., 2018, 2020; Popovic et al., 2009; Somer et al., 2013; Soskic et al., 2012, 2016; Todorović, 2003; Todorović and Nikolic, 2000).

The optimization of the model is pursued, where only dominant processes in the measurement range are to be accounted for, since more detailed models, which include (too) many low-influence processes, result in an imprecise determination of the examined structure parameters by inverse problem-solving (Nesic et al., 2018, 2019, 2020, 2022).

In transmission PT/PA measurements, similar to other techniques (AFM, IR-spectroscopy…), additional sample preparation may be required: coatings and layers with desired electronic, optical, or other properties are applied in order to protect the detector and/or to increase measurement SNR (Cruz and Gurevich, 1995; Medina et al., 2002; Muñoz Aguirre et al., 2000)(Astrath et al., 2010; Balderas-López et al., 2002; Mansanares et al., 1991; Ordóñez-Miranda and Alvarado-Gil, 2010). In this case, the examined sample is regarded as a multilayered structure. Experimental consideration and theoretical modeling of these systems, aimed at the characterization of thin films, require simultaneous consideration of the influence of all layers (Cabrera et al., 2015; Korte and Franko, 2015; Markushev et al., 2017; Ordonez-Miranda et al., 2022; Pawlak et al., 2020, 2021). However, in PT methods, the applied high-absorbance layer may be much thinner than the examined thin film, reducing its influence on the effect of the surface absorption heat source as the generator of the measured signal (Galovic et al., 2014; Markushev et al., 2012; Nesic, Galovic, et al., 2012). This way, the required detector protection from the excitation laser radiation is achieved, but the information regarding the optical properties of the examined sample is lost.

A special case, investigated in this paper, is “thin film – very thin optically opaque coating”, whereas the opaque coating (of high absorbance) is not irradiated directly but acts as a surface absorbent, i.e. it forms a surface heat source on the non-illuminated side of the sample. In this measurement position, the coating protects the detector in the transmission configuration, and it does not affect heat transfer but exerts influence on the distribution of optically generated heat sources within the sample. Optical properties of the sample affect the recorded signal due to the formation of volumetric heat source, induced by the EM energy absorption in the sample, which is experimentally confirmed and published result (Miletic et al., 2020, 2022).

In this paper, a theoretical model describing surface temperature variations in the structure defined above is presented. The influence of optical absorption on temperature gradient is examined. Depending on the product of the optical absorption coefficient and sample thickness (optical absorbance), it is shown that an inverse temperature gradient may occur, affecting the direction and magnitude of thermoelastic displacement.

2. THEORETICAL MODELING

PT effect results in heat transfer through the optically excited sample and, thus, space distribution of temperature change within its boundaries is induced. Consequently, a temperature gradient is formed inside the sample, which can cause its thermoelastic bending. This gradient, considering the small thickness of the sample, can be approximated by the relation of temperature variations at the surfaces of the sample.

The geometry of the problem in transmission PT experimental configuration is presented in Figure 1:

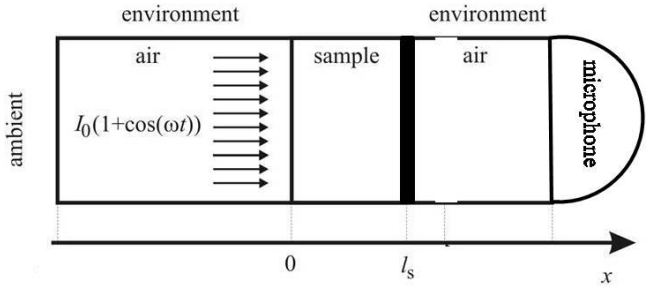

Fig. 1 Experimental set-up: surface absorbent with coating on the non-illuminated side in transmission configuration

The sample is exposed to intensity-modulated optical EM radiation:

$$I(x,t) = \frac{I_0}{2}(1+\cos\omega t), \tag{1}$$

where I_0 is the intensity of the excitation beam at the surface of the sample, given in [W/m^2], ω is the rotational frequency ($\omega = 2\pi f$), given in [s^{-1}]. Absorption of incident energy, in general, is described by Beer – Lamber's law:

$$I_{abs}(x) = (I_0/2)e^{-\beta x}(1+\cos\omega t), \tag{2}$$

where β signifies the coefficient of optical absorption of the medium, given in [m^{-1}].

The generation of heat sources in the volume of the sample is described as:

$$S(x,t) = -\eta\frac{\partial I_{abs}(x,t)}{\partial x}. \tag{3}$$

Based on expressions 2 and 3, for the structure presented in Figure 1, generated heat sources can be described as in the following expression:

$$S(x,t) = \frac{I_0}{2}\left[\eta\beta e^{-\beta x} + e^{-\beta l}\delta(x-l)\right]\cdot[1+\cos\omega t], \tag{4}$$

where η represents the quantum coefficient of conversion of incident energy into heat.

Temperature distribution inside the sample can be expressed as:

$$T(x,t) = T_{amb} + \theta(x) + \vartheta(x,t), \tag{5}$$

where T_{amb} is the temperature of the environment, $\theta(x)$ is the temperature component variable in space, while $\upsilon(x,t)$ represents the temperature component variable in both space and time – the direct consequence of the PT effect.

Given the fact that only the temporal temperature component is of relevance in measurements, the distribution of this dynamic temperature variation can be determined by solving the following system of equations:

$$\left[k\frac{\partial^2}{\partial x^2}-\rho C_P\left(\frac{\partial}{\partial t}+\tau\frac{\partial^2}{\partial t^2}\right)\right]\vartheta(x,t)=-\left(1+\tau\frac{\partial}{\partial t}\right)S(x,t), \tag{6}$$

$$\left(1-\tau\frac{\partial}{\partial t}\right)q(x,t)=-k\frac{\partial\vartheta(x,t)}{\partial t}, \tag{7}$$

with zero boundary conditions (considering air as a much worse heat insulator in comparison to the sample):

$$q(0,t)=0, \tag{8}$$

$$q(l,t)=0. \tag{9}$$

In expressions (6-9), k stands for heat conductivity given in [W/(mK)], C_P is volumetric heat capacity given in [J/(m^{3}K)], D_T=k/C_P represents heat diffusivity given in [m^2/s], and τ is thermal relaxation time given in [s].

The system of partial differential equations is Fourier-transformed into the system of linear non-homogenous differential equations, which takes its form (in the complex domain) as:

$$\frac{d^2\tilde{\vartheta}(x)}{dx^2}-\tilde{\sigma}^2\tilde{\vartheta}(x)=-\frac{1+j\omega\tau}{k}\frac{I_0}{2}\eta\beta e^{-\beta x}, \tag{10}$$

$$\tilde{q}(x)=-\frac{1}{\tilde{\sigma}_s\tilde{z}_c}\frac{d\tilde{\vartheta}(x)}{dx}, \tag{11}$$

with boundary conditions:

$$\tilde{q}(0)=0, \tag{12}$$

$$\tilde{q}(l)=\frac{I_0}{2}e^{-\beta l}, \tag{13}$$

where parameter $\tilde{\sigma}$ represents the complex coefficient of heat propagation, and $\tilde{z}_c$ represent heat impedance, both of which are given as:

$$\tilde{\sigma}=\sqrt{\frac{j\omega(1+j\omega\tau)}{D_T}}, \tag{14}$$

$$\tilde{z}_c=\frac{\sqrt{D_T}}{k}\sqrt{\frac{1+j\omega\tau}{j\omega}}. \tag{15}$$

Herein, $\tilde{\vartheta}(x)$ i $\tilde{q}(x)$ denote complex expressions for dynamic temperature variation and heat flux:

$$\vartheta(x,t)=Re\{\tilde{\vartheta}(x)e^{-j\omega t}\}, \tag{16}$$

$$q(x,t)=Re\{\tilde{q}(x)e^{-j\omega t}\}. \tag{17}$$

Solving the system of differential equations defined above, final expressions for surface temperature variations of the examined sample are obtained:

$$\vartheta(0)=\frac{I_0 z_c}{2\cdot\sinh(\sigma l_s)}\cdot\frac{1}{\sigma^2-\beta^2}\cdot\left[\sigma\beta\sinh(\sigma l_s)-\beta^2\cosh(\sigma l_s)+\sigma^2 e^{-\beta l_s}\right], \tag{18}$$

$$\vartheta(l_s)=\frac{I_0 z_c}{2\cdot\sinh(\sigma l_s)}\cdot\frac{1}{\sigma^2-\beta^2}\cdot\left[-\beta^2+(\sigma\beta\sinh(\sigma l_s)+\sigma^2\cosh(\sigma l_s))e^{-\beta l_s}\right]. \tag{19}$$

3. RESULTS AND DISCUSSION

In theoretical considerations, Poly-L-lactide (PLLA) with the following properties, listed in Table 1, was used. The value of the coefficient of absorption, β, is varied with respect to the way of preparation of PLLA thin film, which also determines its level of crystallinity (Miletic et al., 2020). The thickness of the thin opaque coating (absorption layer) is considered much smaller, while its coefficient of optical absorption is considered much higher in comparison to the same properties of the examined PLLA. The quantum conversion coefficient is considered equal to one, aiming at computational simplicity.

Table 1 Examined material properties

Parameter	Value
$k\left[\frac{W}{mK}\right]$	0.13
$D_T\left[\times 10^{-8}\frac{m^2}{s}\right]$	5.8
$\beta\left[\frac{1}{m}\right]$	500 – 9000
$l_s\,[\times 10^{-6}m]$	30 – 300

Changing the sample thickness at fixed values of β, the following surface temperature variation characteristics are acquired (Figure 2):

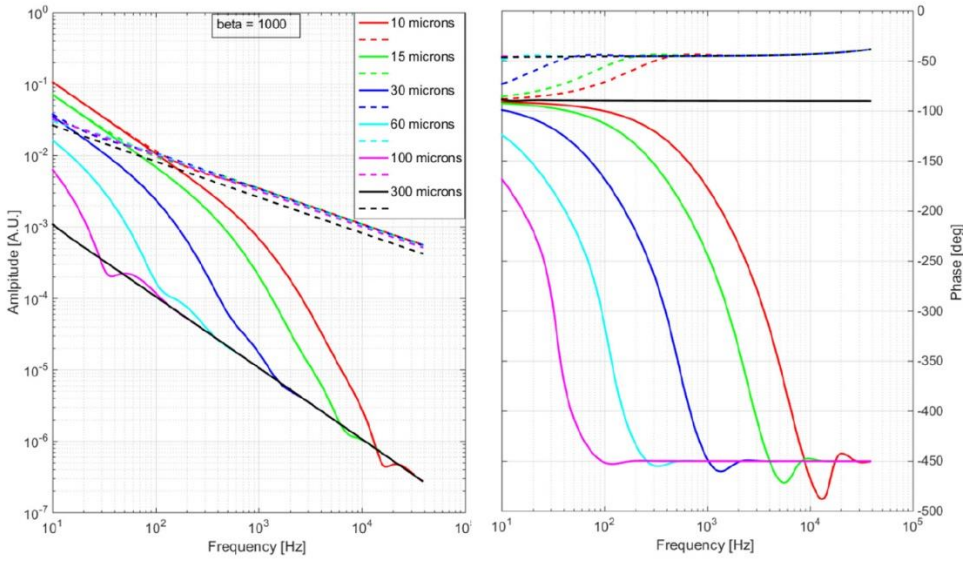

(a) (b)

Fig. 2 Variation of l_s = (10,15,30,60,100,300) μm at fixed value of β = *1000* m^{-1}

With regard to the amplitude characteristics, at a fixed value of the optical coefficient of absorption (β = *1000* m^{-1}), the increase in sample thickness (l_s) results in a slight

temperature variation decrease at the non-illuminated side (dotted lines). On the other hand, at the illuminated side, a considerable shape alteration (full lines) can be observed: firstly, a well-defined local minimum point is shifted towards lower frequencies, simultaneously becoming less and less pronounced, while a new local minimum point emerges (always at lower frequency); and secondly, the line becomes more and more flat and monotonously decreasing. Its final shape is given in the full black line of Figure 2-a.

With regard to the phase, the increase in sample thickness results in the increase of slope at the non-illuminated side (in a limited frequency range), but also in the shift towards lower frequencies of the point where phase lines get asymptotically close. On the other hand, at the illuminated side (similarly to the behavior of the amplitude characteristic), a local minimum is shifted towards lower frequencies while becoming less pronounced, at the same time.

Overall, looking at Figure 2, it can be observed that the increase in sample thickness results in more flat, monotonously decreasing amplitude lines of constant slope (depending on the side of the sample) at all modulation frequencies. The lines lose peculiarities, such as local minima and/or turning points, and become parallel to each other. Phase lines also become monotonous and get asymptotically close.

It is also important to note that, with the increase of sample thickness, a phenomenon of *temperature gradient inversion* occurs (the intensity of surface temperature variations at the non-illuminated side of the sample becomes higher in comparison to the illuminated side), which is not the case for thin samples at low modulation frequencies.

In Figure 3 amplitude and phase characteristics of surface temperature variations at illuminated and non-illuminated sides of the sample are presented at two thickness levels: l_s = 300μm (a,b) and l_s = 30μm (c,d), for a wide range of coefficient of optical absorption (β=500-9000 m^{-1}).

At $l_s = 300\ \mu m$, with regard to amplitude (Figure 3-a), the decrease of β results in the increase of temperature variation at the non-illuminated and the increase at the illuminated side of the sample. At the high value of β = 9000 m^{-1}, there exists a frequency above which the effect of temperature gradient inversion takes place, however with its decrease ($\beta <$ 6000 m^{-1}), this effect is present in the whole frequency range.

At $l_s = 30\ \mu m$ (Figure 3-c), the influence of β alteration is more observable at the illuminated surface and high frequencies, while at low frequencies it is lost completely at both sides. At the lowest frequencies, the lines get asymptotically close, i.e. surface temperature variations at both surfaces become equal and, consequently, the temperature gradient becomes zero. Also, the decrease of β results in the soothing and shifting towards higher frequencies of a local minimum, until it becomes completely lost, while at the same time, at a certain (fixed) modulation frequency, another local minimum point is formed.

The decrease of temperature variation at the non-illuminated side is more easily observable at higher sample thickness, (Figure 3-a, l_s = 300 μm, in comparison to Figure 3-c, l_s = 30 μm). Also, the lines are distinctly separated, i.e. there exists a temperature gradient in the whole frequency range (in comparison to the lower thickness, where lines get asymptotically close at low frequencies, and thus the temperature gradient is negligible).

With regard to the phase lines, at both surfaces, they tend to get asymptotically close, although at high thickness the effect of β alteration is more easily observable (in comparison to thinner sample, Figures 3-b and 3-d). With the increase of β, on the irradiated side, certain soothing of the local minimum occurs, but its position on frequency axes remains the same. At lower frequencies, the slope of lines is dependable on the coefficient

of optical absorption. Also, with the increase of β temperature variation phase on the irradiated side increases and on the non-irradiated side decreases, similar to amplitude lines, which is more notable at higher thickness levels.

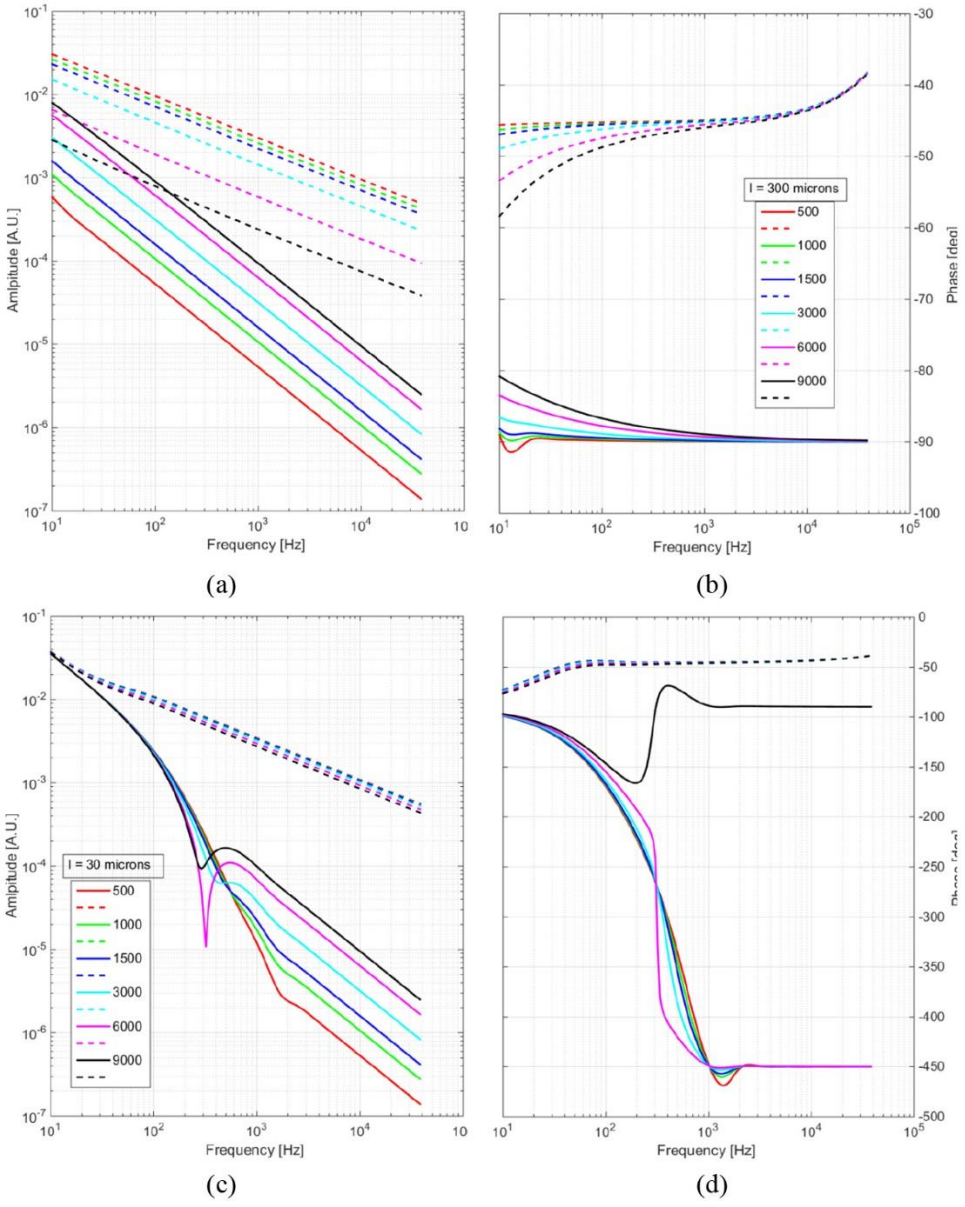

Fig. 3 Influence of varying β (500,1000,1500,3000,6000,9000) m^{-1} at two levels of l_s (300 µm,30 µm)

The effect of temperature variation inversion, and consequently the temperature gradient inversion, at low thickness levels, is present in the whole range of modulation frequencies. Also, one can note that this effect increases with the decrease of the optical absorption coefficient.

Based on amplitude characteristics of surface temperature variations presented in Figures 2 and 3, it can be concluded that at the high thickness level of the sample, along with a simultaneous increase in the coefficient of optical absorption, the effect of the inversion of surface temperature variations takes place at least in one region of modulation frequency range. Since, in theoretical modeling, sample thickness and the coefficient of optical absorption figure in the form of a product (in several instances), the whole model can be transformed in a way that this product is separately accounted for, in the form of a parameter. This parameter is known as the *absorbance of the sample*, e_1, and is given in the following form:

$$e_1 = \beta l_S, \tag{20}$$

while the introduction of the replacement parameters:

$$a = \sigma l_S, \tag{21a}$$

$$P_1 = \frac{S_0 z_C F}{\sinh(a)} \cdot \frac{1}{a^2 - {e_1}^2}, \tag{21b}$$

transforms the expressions (18) and (19) into the following form:

$$\vartheta(0) = P_1(a e_1 \sinh a - {e_1}^2 \cosh a + a^2 e^{-e_1}), \tag{22}$$

$$\vartheta(l_S) = P_1[-{e_1}^2 + (e_1 a \sinh a + a^2 \cosh a) e^{-e_1}]. \tag{23}$$

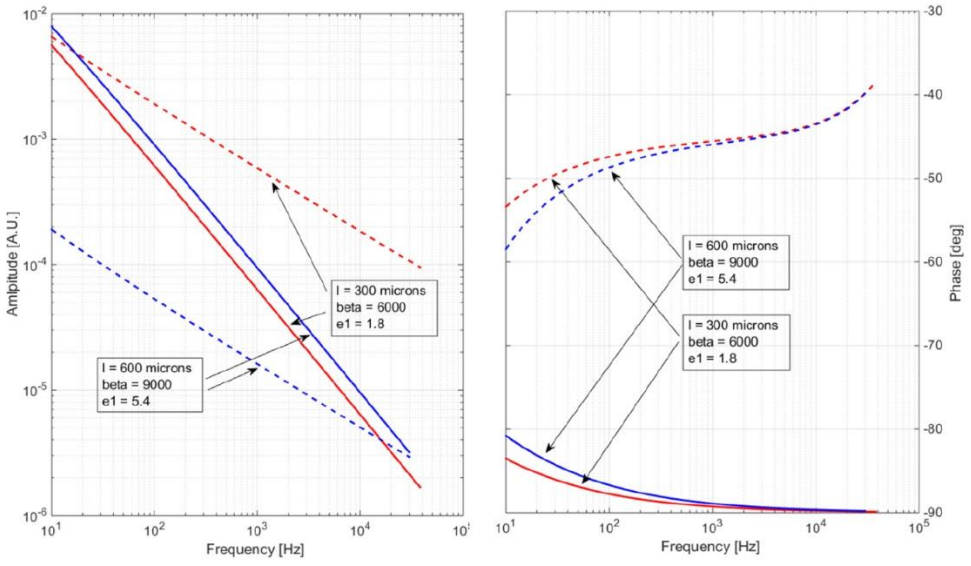

(a) (b)

Fig. 4 The influence of different values of absorbance (e_1) on amplitude (a) and phase (b) of surface temperature variations of the examined sample

The noted effect of temperature (variation, but also the gradient) inversion as the function of e_1 can be illustrated in Figure 4. The minimum value of absorbance when the inversion of temperature gradient occurs (at lowest frequencies) is $e1\_min$ = 1.8, while its value when the phenomenon is present in the whole frequency range is approximately $e1$ = 5.4.

Temperature gradient induced by the photothermal effect results in thermoelastic bending of the examined sample. In theoretical and experimental papers dealing with the PA response of similar systems, a negative temperature gradient has been reported and modeled (Figure 5-a) at various modulation frequencies. However, in papers dealing with piezoelectric PA spectroscopy (Maliński et al., 2007; Zakrzewski et al., 2017), the phenomenon of temperature gradient inversion has been reported as the consequence of the alteration of the optical coefficient of absorption resulting from the change in excitation EM radiation wavelength (excitation energy) (similar to the effect obtained in this work, only depending on the modulation frequency) which also leads to the change in the direction of thermoelastic bending (Figure 5-b). In contrast to piezoelectric spectroscopy, in modulation frequency–based methods (photoacoustics, PT diffraction, and deflection), the effect of temperature gradient inversion can be present in the whole measurement range, depending on the sample absorbance.

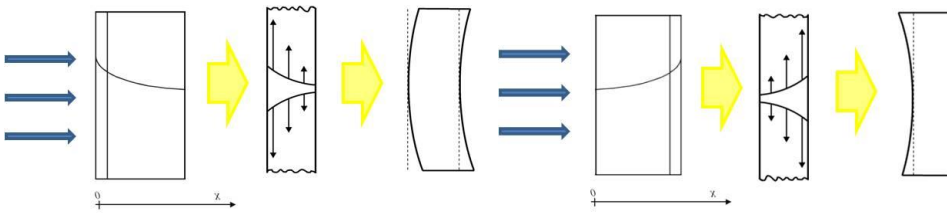

(a) (b)

Fig. 5 Influence of temperature gradient on the thermoelastic displacement of the sample, as a function of the position of the coating (illuminated – a, non-illuminated – b)

CONCLUSION

Detailed analysis of the model has proven that in thin samples with surface absorption of incident EM radiation at a non-illuminated surface and a certain value of optical absorption coefficient, the phenomenon of temperature gradient inversion occurs. Given that thermoelastic displacement is proportional to this gradient, the conclusion is derived that the described gradient change can result in the oscillation of the sample in the direction opposite to the usual case (of surface absorbent on the illuminated side).

The occurrence of the borderline case, where in one part of the modulation frequency range the inversion is not present while in the rest of the range it exists, depends on the coefficient of optical absorption, but also the thickness of the sample.

All of the above indicates the necessity of further theoretical and experimental exploration of the influence of thermoelastic bending on the photoacoustic response of the samples with low levels of absorbance in the configuration “illuminated sample – optically opaque coating”, aimed at determination thermal, elastic and optical properties by methods based on PA response measurement.

Acknowledgement: *This work was supported by the Ministry of Education, Science and Technological Development of the Republic of Serbia, contract No. 451-03-9/2021-14/200017 and No. 451-03-68/2022-14/200124*

REFERENCES

Aleksić, S. M., Markushev, D. K., Markushev, D. D., Pantić, D. S., Lukić, D. V, Popovic, M. N., Galovic, S. P., 2022. Silicon, 14, 9853–9861. doi:10.1007/s12633-022-01723-6

Astrath, N. G. C., Astrath, F. B. G., Shen, J., Lei, C., Zhou, J., Liu, Z. S., Navessin, T., Baesso, M. L., Bento, A. C., 2010. J. Appl. Phys., 107(4), 43514. doi:10.1063/1.3310319

Balderas-López, J. A., Mandelis, A., García, J. A., 2002. J. Appl. Phys., 92(6), 3047–3055. doi:10.1063/1.1500784

Cabrera, H., Mendoza, D., Benitez, J. L., Flores, C. B., Alvarado, S., Marin, E., 2015. J. Phys. D, Appl. Phys., 48(46), 465501. doi:10.1088/0022-3727/48/46/465501

Cruz, G. G. de la, Gurevich, Y. G., 1995. Phys. Rev. B, 51(4), 2188–2192. doi:10.1103/PhysRevB.51.2188

Djordjevic, K. L., Markushev, D. D., Cojbasic, Z. M., Galovic, S. P., 2020. Inverse Probl. Sci. En., 1–15. doi:10.1080/17415977.2020.1787405

Djordjevic, K. L., Milicevic, D., Galovic, S. P., Suljovrujic, E., Jacimovski, S. K., Furundzic, D., Popovic, M. N., 2022. Int. J. Thermophys., 43(5). doi:10.1007/s10765-022-02985-3

Djordjevic, K. L., Markushev, D. D., Ćojbašić, Ž. M., Djordjevic, K. L., 2019. Silicon, 12(6), 1289–1300. doi:10.1007/s12633-019-00213-6

Dramićanin, M. D., Djokovic, V., Galović, S., 2000. J. Phys. D, Appl. Phys., 33(14), 1736–1738. doi:10.1088/0022-3727/33/14/313

Galovic, Kostoski, D., Stamboliev, G., Suljovrujic, E., 2003. Radiat. Phys. Chem., 67(3–4), 459–461. doi: 10.1016/S0969-806X(03)00085-9

Galović, S., Dramićanin, M. D., 1999. J. Phys. D, Appl. Phys., 32(13), 1511–1516. doi: 10.1088/0022-3727/32/13/312

Galovic, S. P., Kostoski, D., 2003. J. Appl. Phys., 93(5), 3063–3070. doi: 10.1063/1.1540741

Galovic, S. P., Soskic, Z. N., Popovic, M. N., Cevizovic, D., Stojanovic, Z., 2014. J. Appl. Phys., 116(2), 0–12. doi:10.1063/1.4885458

Korte, D., Franko, M., 2015. J. Opt. Soc. Am. A, 32(1), 61–74. doi:10.1364/JOSAA.32.000061

Maliński, M., Zakrzewski, J., Strzałkowski, K., 2007. Int. J. Thermophys., 28(1), 299–316. doi:10.1007/s10765-006-0126-2

Mansanares, A. M., Vargas, H., Galembeck, F., Buijs, J., Bicanic, D., 1991. J. Appl. Phys., 70(11), 7046–7050. doi:10.1063/1.349782

Markushev, D. D., Ordonez-Miranda, J., Rabasovic, M. D., Chirtoc, M., Todorović, D. M., Bialkowski, S. E., Korte, D., Franko, M., 2017. Eur. Phys. J. Plus, 132(33), 1–9. doi:10.1140/epjp/i2017-11307-2

Markushev, D. K., Markushev, D. D., Aleksić, S., Pantić, D. S., Galovic, S. P., Todorovic, D. M., Ordonez-Miranda, J., 2019. J. Appl. Phys., 126(18), 185102. doi:10.1063/1.5100837

Markushev, Dragan D., Rabasovic, M. D., Nesic, M. V., Popovic, M. N., Galovic, S. P., Rabasovic, M. D., 2012. Int. J. Thermophys., 33(10–11), 2210–2216. doi:10.1007/s10765-012-1229-6

Markushev, Dragana K., Markushev, D. D., Aleksić, S. M., Pantić, D. S., Galovic, S. P., Todorovic, D. M., Ordonez-Miranda, J., 2020. J. Appl. Phys., 128(9), 095103. doi:10.1063/5.0015657

Markushev, Dragana K., Markushev, D. D., Galovic, S. P., Aleksic, S., Pantic, D., Todorovic, D. M., 2018. Facta Universitatis - Series: Electronics and Energetics, 31(2), 313–328. doi:10.2298/fuee1802313m

Medina, J., Gurevich, Y. G., Logovinov, G. N., Rodriguez, P., Cruz, G. G. de la., 2002. Mol. Phys., 100(19), 3133–3138. doi:10.1080/00268970210139877

Miletic, V. V., Djordjevic, K. L., Markushev, D. D., Popovic, M. N., Galovic, S. P., Milicevic, D., Nesic, M. V., 2020. Photoacoustic Characterization of PLLA Samples At Different Crystallinity Levels, (Fotoakustička karakterizacija PLLA uzoraka različitih nivoa kristaliničnosti). 19th International Symposium INFOTEH-JAHORINA, 18-20 March 2020, 109–113. https://infoteh.etf.ues.rs.ba/zbornik/2020/radovi/P-2/P-2-1.pdf

Miletic, V. V., Markushev, D. D., Markushev, D. K., Popovic, M. N., Djordjevic, K. L., Galovic, S. P., Nesic, M. V., 2022. Ispitivanje uticaja nanetog sloja boje na površinske temperaturske varijacije laserski sinterovanog poliamida. 21st International Symposium INFOTEH-JAHORINA, 16-18 March 2022, March, 16–18. https://infoteh.etf.ues.rs.ba/zbornik/2022/

Muñoz Aguirre, N., Cruz, G. G. de la, Gurevich, Y. G., Logvinov, G. N., Kasyanchuk, M. N., 2000. Phys. Status Solidi B, 220(1), 781–787. doi:10.1002/1521-3951(200007)220:1<781::AID-PSSB781>3.0.CO;2-D

Nesic, M. V., Galovic, S. P., Soskic, Z. N., Popovic, M. N., Todorović, D. M., 2012. Int. J. Thermophys., 33(10–11), 2203–2209. doi:10.1007/s10765-012-1237-6

Nesic, M. V., Gusavac, P., Popovic, M. N., Soskic, Z. N., Galovic, S. P., 2012. Phys. Scripta, T149(T149), 014018. doi:10.1088/0031-8949/2012/T149/014018

Nesic, M. V., Popovic, M. N., Djordjevic, K. L., Miletic, V. V., Jordovic-Pavlovic, M. I., Markushev, D. D., Galovic, S. P., 2020. Opt. Quant. Electron., 53(7), 381. doi:10.21203/rs.3.rs-267516/v1
Nesic, M. V., Popovic, M. N., Galovic, S. P., 2016. Opt. Quant. Electron., 48(290), 7. doi:10.1007/s11082-016-0564-4
Nesic, M. V., Popovic, M. N., Galovic, S. P., 2019. Atoms, 7(1), 24. doi:10.3390/atoms7010024
Nesic, M. V., Popovic, M. N., Galovic, S. P., Djordjevic, K. L., Jordovic-Pavlovic, M. I., Miletic, V. V., Markushev, D. D., 2022. J. Appl. Phys., 131(10). doi:10.1063/5.0075979
Nesic, M. V., Popovic, M. N., Rabasovic, M., Milicevic, D., Suljovrujic, E., Markushev, D., Stojanovic, Z., 2018. Int. J. Thermophys., 39(2). doi:10.1007/s10765-017-2345-0
Ordóñez-Miranda, J., Alvarado-Gil, J. J., 2010. Int. J. Ther. Sci., 49(1), 209–217. doi:10.1016/j.ijthermalsci.2009.07.005
Ordonez-Miranda, J., Anufriev, R., Nomura, M., Volz, S., 2022. Phys. Rev. B, 106(10), L100102. doi:10.1103/PhysRevB.106.L100102
Park, H. K., Grigoropoulos, C. P., Tam, A. A. C., 1995. Int. J. Thermophys., 16(4), 973. doi: 10.1007/BF02093477
Pawlak, M., Jukam, N., Kruck, T., Dziczek, D., Ludwig, A., Wieck, A. D., 2020. Measurement, 166, 108226. doi:10.1016/j.measurement.2020.108226
Pawlak, M., Kruck, T., Spitzer, N., Dziczek, D., Ludwig, A., Wieck, A. D., 2021. Appl. Sci., 11(13). doi:10.3390/app11136125
Popovic, M. N., Galovic, S. P., Stojanovic, Z., 2009. Acta Phys. Pol. A, 116(4), 535–537. doi: 10.12693/APhysPolA.116.535
Popovic, M. N., Nesic, M. V., Markushev, D. D., Jordovic-Pavlovic, M. I., Galovic, S. P., 2021. J. Appl. Phys.. doi:10.1063/5.0015898
Popovic, M. N., Nesic, M. V., Zivanov, M., Markushev, D. D., Galovic, S. P., 2018. Opt. Quant. Electron., 50(9), 1–10. doi:10.1007/s11082-018-1586-x
Rosencwaig, A., Gersho, A., 1975. Science, 190, 556–557. doi:10.1126/science.190.4214.556
Rosencwaig, A., Gersho, A., 1976. J. Appl. Phys., 47(1), 64–69. doi: 10.1063/1.322296
Sablikov, V. A., Sandomirskii, V. B., 1983. Phys. Status Solidi A, 120, 471. doi: 10.1002/pssb.2221200203
Somer, A., Camilotti, F., Costa, G. F., Bonardi, C., Novatski, A., Andrade, A. V. C., Kozlowski, V. A., Cruz, G. K., 2013. J. Appl. Phys., 114(6). doi:10.1063/1.4817655
Soskic, Z. N., Ciric-Kostic, S., Galovic, S. P., 2016. Int. J. Therm. Sci., 109, 217–230. doi:10.1016/j.ijthermalsci.2016.06.005
Soskic, Z. N., Galovic, S. P., Bogojevic, N., Todosijevic, S., 2012. Facta Universitatis - Series: Electronics and Energetics, 25(3), 213–224. doi:10.2298/fuee1203213s
Tam, A. A. C., 1986. Rev. Mod. Phys., 58, 381–431. doi: 10.1103/RevModPhys.58.381
Todorović, D. M., 2003. Rev. Sci. Inst., 74(1), 582–585. doi:10.1063/1.1523133
Todorović, D. M., Nikolic, P. M., 2000. Carrier transport Contribution on Thermoelastic and Electronic Deformation in Semiconductors. In A. Mandelis, P. Hess (Eds.), Progress in Photothermal and Photoacoustic Science and Technology - Semiconductors and Electronic Materials (Vol. 4, pp. 271–315). SPIE Press, Bellingham.
Vargas, H., Miranda, L. C. M., 1988. Phys. Rep., 161, 43–101. doi:10.1016/0370-1573(88)90100-7
Zakrzewski, J., Maliński, M., Chrobak, Pawlak, M., 2017. Int. J. Thermophys., 38(2). doi:10.1007/s10765-016-2137-y

UTICAJ OPTIČKOG APSORBERA POSTAVLJENOG NA NEOBASJANU POVRŠINU TANKOG FILMA NA TEMPERATURNI GRADIJENT INDUKOVAN FOTOTERMALNIM EFEKTOM

U radu je prikazan model koji opisuje površinske temperaturske varijacije nastale kao posledica fototermalnog efekta u strukturi tanki film – prevlaka sa visokim koeficijentom optičke apsorpcije, gde je obasjan tanki film. Analiziran je uticaj koeficijenta optičke apsorpcije i debljine uzorka na indukovani gradijent temperature. Pokazano je da u zavisnosti od proizvoda koeficijenta optičke apsorpcije i debljine uzorka (apsorbanse uzorka), u takvoj strukturi može doći do formiranja inverznog temperaturskog gradijenta, što utiče na smer i veličinu termoelastičnog pomeraja.

Ključne reči: *Fototermalni odziv, fotoakustika, termoelastično savijanje, uzorci niske apsorbanse*